AMP Kinase Promotes Bcl6 Expression in both Mouse and Human T cells

Markus M. Xie, Tohti Amet, Hong Liu, Qigui Yu,

and Alexander L. Dent[1]

Department of Microbiology and Immunology, Indiana University School of Medicine, Indianapolis, Indiana, USA.

Corresponding author: Alexander Dent

317-274-7524 (phone)

317-274-7582 (FAX)

adent2@iupui.edu

RUNNING TITLE: Control of Bcl6 by AMPK

This is the author's manuscript of the article published in final edited form as:

Xie, M. M., Amet, T., Liu, H., Yu, Q., & Dent, A. L. (2016). AMP kinase promotes Bcl6 expression in both mouse and human T cells. Molecular immunology, 81, 67. https://doi.org/10.1016/j.molimm.2016.11.020

ABSTRACT

The transcription factor Bcl6 is a master regulator of follicular helper T (T_{FH}) cells, and understanding the signaling pathway that induces Bcl6 and T_{FH} cell differentiation is therefore critical. IL-2 produced during T cell activation inhibits Bcl6 expression but how T_{FH} cells evade IL-2 inhibition is not completely understood. Here we show that Bcl6 is highly up-regulated in activated CD4 T cells following glucose deprivation (GD), and this pathway is insensitive to inhibition by IL-2. Similar to GD, the glucose analog 2-deoxyglucose (2DG) inhibits glycolysis, and 2DG induced Bcl6 expression in activated CD4 T cells. The metabolic sensor AMP kinase (AMPK) is activated when glycolysis is decreased, and the induction of Bcl6 by GD was inhibited by the AMPK antagonist compound C. Additionally, activation of AMPK by the drug AICAR caused Bcl6 up-regulation in activated CD4 T cells. When mice were immunized with KLH using AICAR as an adjuvant, there was a strong T_{FH}–dependent enhancement of KLH-specific antibody (Ab) responses, and higher Bcl6 expression in T_{FH} cells *in vivo*. Activation of AMPK strongly induced BCL6 and the up-regulation of T_{FH} cell marker expression by human CD4 T cells. Our data reveal a major new pathway for T_{FH} cell differentiation, conserved by both mouse and human T cells. Mature T_{FH} cells are reported to have a lower metabolic state compared to T_H1 cells. Our data indicates that decreased metabolism may be deterministic for T_{FH} cell differentiation, and not simply a result of T_{FH} cell differentiation.

1. Introduction

Follicular T helper (T_{FH}) cells help B cells form germinal centers (GCs) and produce high-affinity antibodies (Abs) (Fazilleau et al. 2009; Crotty et al. 2010). T_{FH} cells control the initiation as well as the outcome of the GCB cell response (Breitfeld et al. 2000; Schaerli et al. 2000; Vinuesa et al. 2005; McHeyzer-Williams et al. 2009). Thus, T_{FH} cells are critical for the proper production of protective Abs during an infection. However the over-production of T_{FH} cells can also lead to autoimmunity, since excess T_{FH} cell activity can help self-reactive B cells to produce auto-Abs (Vinuesa et al. 2005; Odegard et al. 2008; Linterman et al. 2009). Understanding the proper regulation of T_{FH} cell differentiation is essential for devising strategies that either promote beneficial Ab responses or prevent Ab-mediated autoimmune diseases.

Bcl6 is a transcriptional repressor that is essential for the development and stability of T_{FH} cells (Johnston et al. 2009; Nurieva et al. 2009; Yu et al. 2009; Crotty 2011; Hollister et al. 2013). How Bcl6 expression is induced to promote T_{FH} cell differentiation has been the subject of much interest, and can be driven by STAT factor transcription following signaling by cytokines such as IL-6 and IL-12 (Poholek et al. 2010; Crotty 2011; Schmitt et al. 2014). The stable activation of Bcl6 expression in CD4 T cells during T_{FH} cell differentiation has to overcome two critical impediments: 1) Bcl6 strongly auto-represses its own expression (Pasqualucci et al. 2003; Mendez et al. 2008), and 2) IL-2 produced during T cell activation inhibits Bcl6 expression (Ballesteros-Tato et al. 2012; Johnston et al. 2012; Nurieva et al. 2012; Oestreich et al. 2012; Liao et al. 2014). T_{FH}-like cells can be generated *in vitro* with human CD4 T cells and STAT3/STAT4-activating cytokines plus TGFβ (Schmitt et al. 2014). However, these same signals do not promote mouse T_{FH} cell differentiation *in vitro*, and in particular, TGFβ plays different roles in mouse versus human CD4 T cell differentiation (Schmitt et al. 2014). Recently, Cyster and colleagues found that during an immune response, dendritic cells (DCs) can up-regulate expression of the IL2 receptor (IL2R) in order to compete with IL-2 signaling by CD4 T cells and this promotes T_{FH} cell differentiation (Li et al. 2016). While this DC-IL2R mechanism

appears to be important for early T_{FH} cell differentiation, much work remains to understand the relevance of this pathway in different immune settings. Another mechanism for blocking IL-2 *in vivo* to promote T_{FH} cell differentiation involves IL2R-expressing regulatory T (Treg) cells (Leon et al. 2014). The significance of this pathway in different immune settings is also unclear. Another potential pathway for controlling IL-2 during the T cell response is through glycolysis, since decreased glycolysis leads to decreased IL-2 translation (Chang et al. 2013).

Because of the complexity of Bcl6 regulation as noted above, the potential for regulation of IL-2 expression via glycolysis (Chang et al. 2013) and the fact that T_{FH} cells have an unusual state of low metabolism for effector T cells (Ray et al. 2015), we pursued the idea that Bcl6 expression and T_{FH} cell differentiation is uniquely controlled by metabolic signals. We now report a pathway for the regulation of Bcl6 controlled by the metabolic sensor AMPK. This pathway overrides, or is downstream of, the inhibitory effect of IL-2 on Bcl6 expression. Our new data indicate that metabolic cues during T cell activation can determine whether an activated CD4 T cell can become a T_{FH} cell versus another type of effector T helper cell. Importantly, the AMPK-BCL6 pathway is shared by mouse and human CD4 T cells, revealing a new evolutionarily conserved pathway for T_{FH} cell differentiation.

2. Results

Bcl6 is regulated by glycolysis. Since blocking glycolysis during T cell activation results in an inhibition of cytokine mRNA translation, such that secretion of IFNγ and IL-2 is markedly decreased (Chang et al. 2013), we reasoned that blocking glycolysis might play a role during T_{FH} differentiation, by blocking inhibitory IL-2. Initially, as in Chang *et al* (Chang et al. 2013), we activated wild-type (WT) naïve CD4 T cells in glucose versus galactose medium, but we did not observe significant differences in *Bcl6* expression (data not shown). However, as a control, we also activated naïve CD4 T cells in medium without added glucose or galactose, and analyzed *Bcl6* mRNA expression by QPCR. As shown in Figure 1A, compared to T cells activated in 25 mM glucose, *Bcl6* was increased over 20-fold when the T cells were activated in the absence of added glucose. This was accompanied by an up-regulation of Bcl6 protein, as measured by intracellular staining and flow cytometry (Fig. 1B). We tested if a transformed T cell line showed this same regulation of Bcl6 by glucose withdrawal, and so we tested the EL4 lymphoma cell line by culturing the cells with glucose or without glucose. We observed a similar high increase in *Bcl6* mRNA after 48 h in glucose-deprived conditions, and protein was increased as well as analyzed by flow cytometry (Fig. 1 C, D). Using Cell Trace Violet (CTV)-labeling, we found that Bcl6 was preferentially increased in the no glucose condition compared to the glucose added condition, although there was significantly less cell division without glucose (Suppl. Fig. 1). We then tested the effect of the non-metabolizable glucose analogue 2-deoxyglucose (2DG) when it was added to naïve CD4 T cells activated in DMEM medium containing glucose. As shown in Figure 1E, Bcl6 mRNA increased over 4-fold when metabolism of the normal glucose in the culture is inhibited by 2DG. Because the effect of complete glucose deprivation (GD) on Bcl6 induction was much stronger than the effect with 2DG, we chose to focus on GD for further studies. Note, our medium contains glutamine that can be used as an alternative energy source for T cells (Wang et al. 2011; Blagih et al. 2015), though there is

increased cell death and decreased proliferation in the absence of glucose. We wondered if glucose withdrawal was inhibiting T cell activation, therefore we analyzed IL-2 (*Il2)* and IL-2 receptor alpha (*Il2ra*) chain gene expression. As shown in Figure 2, in the absence of glucose, naïve CD4 T cells still become activated to transcribe levels of *Il2* and *Il2ra* mRNAs comparable to with glucose conditions. However, consistent with published findings that inhibition of glycolysis leads to a block in cytokine translation (Chang et al. 2013), IL-2 was secreted at significantly lower levels in T cells activated under GD conditions than under plus glucose conditions (Fig. 2C). Nonetheless, substantial levels of IL-2 were still secreted under GD conditions (Fig. 2C).

Regulation of Bcl6 by glucose is largely independent from inhibition by IL-2. We wondered if the decreased IL-2 in the GD conditions was leading to the increased Bcl6 levels. We then tested whether adding exogenous IL-2 could down-regulate the induction of Bcl6 in T cells seen with GD, by supplementing the GD cultures with high levels of recombinant human IL-2. However, the added IL-2 had no effect on Bcl6 (Fig. 3A). Since it is difficult to determine if the added human IL-2 was added to an inhibitory level equivalent to that made by T cells in Glu added conditions, we sought another approach to test this question. In order to stringently test the role of IL-2 in the GD effect on Bcl6, we used T cells from IL-2-deficient (KO) mice. When activated *in vitro*, IL-2 KO T cells have a higher level of Bcl6 expression than WT T cells, likely due to their inability to produce IL-2 (data not shown). We then activated naïve CD4 T cells from IL-2KO mice in plus glucose or GD conditions (Fig. 3B). When IL-2 was added to the IL-2 KO T cells activated in plus glucose conditions, Bcl6 was sharply decreased, whereas addition of a similar amount of IL-2 to IL-2 KO T cells activated in GD conditions did not significantly decrease Bcl6 expression (Fig. 3B). These data indicate that the activating effect of GD on Bcl6 expression is dominant over the inhibition by IL-2.

Up-regulation of Bcl6 by glucose deprivation can occur in a secondary stimulation setting. One pitfall of Bcl6 induction by GD is that lack of glucose during T cell activation

prevents the strong T cell expansion that normally occurs during antigen stimulation *in vivo*. We therefore wondered if we could induce Bcl6 by GD in a secondary stimulation, after an initial stimulation and expansion in glucose-containing media. We thus conducted an experiment where naïve CD4 T cells were activated in plus glucose media, and then after 2 days, collected, washed, and re-activated under either plus glucose or GD conditions. As shown in Figure 4A, *Bcl6* transcript is strongly induced in secondary stimulation under GD conditions. The transcript for the activation/T_{FH} marker PD-1 (*Pdcd1*) was strongly up-regulated under GD conditions along with Bcl6 (Fig. 4B), and the key T_{FH} marker *Cxcr5* was also increased in GD conditions compared to plus glucose (data not shown). Notably, the transcript for Blimp-1 (*Prdm1*) was not markedly increased (Fig. 4C), showing specificity for the GD effect. We then stained cells cultured in the secondary stimulation condition for Bcl6 (Fig. 4D, E), Tbet (Fig. 4F) and Foxp3 (Fig. 4G), and found that only Bcl6 was increased following GD. This data shows that key parts of the T_{FH} cell profile (Bcl6 and PD-1) can be induced during an ongoing T cell response, if glucose in the immune environment is depleted while T cells are still being stimulated through the TCR. These results therefore indicate a novel, metabolically-regulated pathway for T_{FH} cell differentiation during the immune response.

Bcl6 and the T_{FH} response is regulated by AMP kinase. Next, we wanted to explore the signaling pathway that leads to induction of Bcl6 expression after GD. The major metabolic sensor for GD is AMP kinase (AMPK), which is activated by elevated AMP levels (Carling 2004; Hardie 2007). Several drugs have been developed that target AMPK, compound C is a small molecule inhibitor of AMPK activity, and the AMP analog AICAR activates AMPK (Zhou et al. 2001; Vincent et al. 2015). We thus tested the activity of AMPK in regulating *Bcl6* expression using these drugs. As shown in Figure 5A, naïve CD4 T cells secondarily activated under GD conditions induce strong Bcl6 expression as expected, but this up-regulation of *Bcl6* can be reversed by compound C treatment. Furthermore, AICAR stimulates significant *Bcl6* expression in naïve CD4 T cells secondarily activated (Fig. 5B) in the presence of glucose. AICAR

stimulation was also able to induce higher *Bcl6* expression under "T_{FH}" culture conditions that block IL-2 and increase the expression of *Bcl6* and T_{FH} markers such as Cxcr5 and Pdcd1. Taken together, these data indicate that AMPK has key role in *Bcl6* regulation in CD4 T cells and may play a role in induction of the T_{FH} phenotype. Previously, AMPK was shown to positively regulate *BCL6* transcription in human endothelial cells, by a mechanism involving inactivation of PARP1 (Gongol et al. 2013). To our knowledge, the data here is the first data linking Bcl6 and AMPK in T cells. Previously, it was shown that AICAR could act as an adjuvant in mice to enhance Ab responses, however T_{FH} cell responses were not specifically analyzed in this study (Andris et al. 2011). We therefore repeated this experiment, by injecting mice with the antigen Keyhole Limpet Hemocyanin (KLH) either with or without AICAR. As shown in Figure 6A, in wild-type (WT) mice, AICAR significantly enhanced the anti-KLH IgG titer by about 3-fold. We then tested if this Ab response was driven by T_{FH} cells, using T cell specific Bcl6 cKO mice (Hollister et al. 2013). Loss of Bcl6 in T cells completely ablates development of T_{FH} cells and GC B cells. When cKO mice were immunized, the overall Ab response was lower due to lack of a GC B cell response, and AICAR did not boost the Ab response to any degree (Fig 6A). These data indicate that AICAR specifically enhances the T_{FH} cell-dependent Ab response. To more carefully analyze if AICAR affected T_{FH} cells, we analyzed responding T cells in immunized mice at days 3, 7 and 14 after immunization with KLH or KLH plus AICAR. However, AICAR did not significantly enhance the frequency or number of T_{FH} cells induced by immunization (Fig. 6B and data not shown), although the percentage of T_{FH} cells was slightly higher following AICAR. However, we did observe that within the T_{FH} cells, Bcl6 expression was significantly enhanced by AICAR (Figure 6C). This data is consistent with our *in vitro* work showing that AICAR can enhance BCL6 expression. Additionally, AICAR significantly increased the number of GC B cells (Fig. 6D), which may be the result of more potent T_{FH} cell activity due to higher Bcl6 expression, or due to a separate effect of AICAR on B cells.

AMPK regulates BCL6 and T_{FH} markers in human T cells. Since conditions for T_{FH} cell differentiation have been more clearly characterized in human T cells compared to mice (Schmitt et al. 2014), we were curious if our findings with regulation of mouse Bcl6 by AMPK translated to human T cells. We therefore isolated naïve CD4 T cells from human peripheral blood mononuclear cells (PBMC), stimulated them in vitro with anti-CD3/anti-CD28 beads, and added reagents that modulate AMPK activity. We found that 2DG potently up-regulated both *BCL6* and *CXCR5* in human CD4 T cells (Fig. 7A, B). In fact human T cells were extremely sensitive to 2DG compared to mouse cells, such that only 1.25 mM 2DG was effective at increasing BCL6, whereas much higher concentrations of 2DG were required to induce Bcl6 in mouse T cells (Fig. 1E). Nonetheless, this result indicated a similar regulatory pathway might exist for both mouse and human T cells. We then tested AICAR in the human CD4 T cell culture system. Similar to what we observed in mouse T cells, AICAR was effective at significantly inducing BCL6 expression, both at the mRNA (Fig. 7C) and protein (Fig. 7D) level. Unlike with mouse T cells, AICAR induced significant up-regulation of the T_{FH} markers CXCR5 (Fig. 7E) and PD-1 (Fig. 7F). Strikingly, AICAR was more effective at inducing transcription of BCL6 (Fig. 7C) and CXCR5 (Fig. 7E) than when the CD4 T cells were cultured in characterized T_{FH} cell conditions (Schmitt et al. 2014). These data indicate that mouse and human T cells share a common AMPK pathway for inducing BCL6, however it also appears that human CD4 T cells are also more prone to develop into T_{FH}–like cells than mouse CD4 T cells when this pathway is activated.

3. Discussion

T_{FH} cells orchestrate the germinal center reaction and hence control the production of high affinity antibodies to antigen, yet the pathways for how T_{FH} cells develop are not well understood either *in vivo* or *in vitro*. Here we have uncovered a novel mode of inducing the master T_{FH} cell regulator Bcl6 involving the metabolic sensor AMPK. Our work here follows a great deal of recent work showing that effector T cell responses are promoted by glycolysis and AMPK (Wang et al. 2011; Chang et al. 2013; Sukumar et al. 2013; Blagih et al. 2015), however T_{FH} cell responses were not analyzed in these previous studies. Our findings here add a new twist to the metabolic regulation of T cells, and indicate that inhibition of glycolysis, with the resulting activation of AMPK, induces Bcl6 expression, which can promote T_{FH} cell responses. Although previous studies have shown that Bcl6 is positively regulated by AMPK in endothelial cells (Gongol et al. 2013), and that Bcl6 is up-regulated by glucose deprivation (GD) in pancreatic cancer cells (Glauser and Schlegel 2009), our findings here shows that this pathway is operational in CD4 T cells, both in mouse and human, and that this pathway can impact T_{FH} cell differentiation.

Curiously, T_{FH} cells have a unique metabolic profile, with a dampened metabolism compared to other effector T cells (Ray et al. 2015). This decreased metabolism may be due in part because Bcl6 is able to repress genes in the glycolysis pathway (Oestreich et al. 2014). Thus, if Bcl6 suppresses glycolysis, T_{FH} cells should have strongly suppressed glycolysis due to their high expression level of Bcl6. A major unresolved question is how this dampened metabolism contributes to the function of T_{FH} cells. In the GC, B cells present cognate Ag to T_{FH} cells and stimulate the T_{FH} cells through the TCR to allow for elaboration of helper cytokines. T_{FH} cells need to be specifically activated in order to help GC B cells, and it has been proposed that strict control of cytokine secretion by T_{FH} cells is a key aspect of their function (Havenar-Daughton et al. 2016; Wu et al. 2016). How cytokine expression is controlled in T_{FH} cells following interaction with GC B cells presenting cognate Ag is a particularly important question for understanding B cell

selection in the GC. We propose that metabolism is normally dampened in T_{FH} cells specifically to limit the non-specific secretion of cytokines by T_{FH} cells in the GC, and that metabolism is transiently activated in T_{FH} cells that are stimulated by cognate GC B cells. Whether the glucose concentration in the GC micro-environment influences this sort of on-off regulation of T_{FH} cell metabolism is an interesting question that warrants further study.

Previous studies have found that Bcl6 is induced by AMPK in endothelial cells (Gongol et al. 2013), and that Bcl6 is up-regulated following glucose deprivation (GD) in pancreatic cancer cells (Glauser and Schlegel 2009), these studies presented different mechanisms for how Bcl6 is induced. In the endothelial cell study, AMPK was shown to inactivate PARP1, which normally represses BCL6 (Gongol et al. 2013), and thus AMPK signaling relieves repression on BCL6. In the glucose deprivation study, activated Foxo1 was shown to induce Bcl6 expression (Glauser and Schlegel 2009). We showed many years ago that Foxo4 positively regulates Bcl6 (Tang et al. 2002), and AMPK can regulate multiple Foxo factors (Nystrom and Lang 2008). Interestingly, Foxo1 was shown to repress early T_{FH} cell differentiation, but also was required for maximal Bcl6 expression and full T_{FH} cell differentiation (Stone et al. 2015). Overall, it is likely that the regulatory pathway for how AMPK activates BCL6 is complex and involves several downstream transcription factors that respond to metabolic signals. While Foxo factors are well-known for responding to metabolic signals and for regulating metabolism, PARP-1 is also responsive to the metabolic state of the cell, as it utilizes the metabolic product NAD+ for its enzymatic function (Luo and Kraus 2012).

Although we found Bcl6 was strongly induced when glycolysis was inhibited, inhibition of glycolysis is also detrimental to T cell activation and proliferation (Wang et al. 2011; Chang et al. 2013; Sukumar et al. 2013; Blagih et al. 2015; Yin et al. 2015; Yin et al. 2016; Zeng et al. 2016). Thus, during a strong T cell proliferative response, abundant glucose is required, and it is unlikely that Bcl6 will be activated by low energy signals through AMPK during a highly proliferative T cell response. Furthermore AMPK appears to be inhibitory to T_{FH} cell responses (Ramiscal et al.

2015). However, we think it is critical to distinguish early T cell activation and expansion from T_{FH} cell differentiation that occurs later in the response. We hypothesize that during a strong T cell response, glucose can be depleted locally, and this can lead to Bcl6 activation via AMP activated AMPK. Indeed, we showed that Bcl6 was induced by glucose deprivation, following an initial T cell activation in the presence of glucose (Figure 4). Although it remains to be tested *in vivo*, this is a plausible pathway for the development of T_{FH} cells during an active immune response, and critically, it is a way for T_{FH} cells to develop in the presence of inhibitory IL-2. Thus, experiments using different types of cKO mice where glucose metabolism is inhibited during T cell activation may give misleading results about the effect of T_{FH} cell responses, when really the effect is on early T cell activation. Similarly cKO mice for AMPK may show augmented T_{FH} cell responses because early T cell activation is increased due to loss of inhibitory activity of AMPK at that stage (Ramiscal et al. 2015).

The fact that Bcl6 represses glycolysis (Oestreich et al. 2014), makes the activation of Bcl6 transcription by glucose deprivation, where glycolysis cannot occur, remarkable. This expression pathway indicates that Bcl6 may be part of an important feedback loop used by the cell to shut off glycolysis, which uses glucose, when glucose is in short supply. This potential regulatory circuit is highly novel and will be pursued in future research. Whether induction of Bcl6 by AMPK has different effects on glycolysis in glucose deprivation conditions versus when glucose is present is another important issue for future investigation.

Ultimately, these findings have significant therapeutic potential, since targeting AMPK by pharmaceutical agents can be used for augmenting T_{FH} cells during vaccination, or for inhibiting T_{FH} cells in an auto-immune disease setting.

4. Materials and Methods

Mice and immunizations. C57BL/6J mice were obtained from Jackson labs and then bred in house. $Bcl6^{fl/fl}$ mice (Hollister et al. 2013) were backcrossed to CD4-cre transgenic mice (Lee et al. 2001) and the C57BL/6 strain for at least six generations. IL-2 knockout mice were obtained from Jackson labs. Mice were bred under specific pathogen-free conditions at the laboratory animal facility at Indiana University School of Medicine and were handled according to protocols approved by the Indiana University School of Medicine Institutional Animal Use and Care Committee (IACUC). For NP-KLH immunization, mice were intraperitoneally (i.p.) injected with 100 μg NP (27) -KLH (Biosearch Technologies) and were sacrificed at the indicated day. For AICAR NP-KLH immunization, 5-10 mg AICAR (Sigma-Aldrich) was mixed with 100 μg NP (27) –KLH in PBS and the mixture was injected i.p., similarly to Andris et al (Andris et al. 2011).

Mouse T cell culture. Naïve CD4 T cells were isolated from the spleen via isolation kit (Miltenyi Biotec). Cells were activated with plate-bound anti-CD3 (10 μg/ml; 145-2C11; Bio X Cell) and anti-CD28 (10 μg/ml; 37.51; Bio X Cell) for 72 h in culture medium, at 1 X 10^6 cells/ml. Glucose-free culture medium was glucose-free DMEM media (Gibco/LifeTechnologies) supplemented with 10% dialyzed FBS, Penicillin/Streptomycin, glutamine, non-essential amino acids, 10 mM HEPES and 55 uM β-mercaptoethanol. Control culture medium was regular DMEM media (Gibco/LifeTechnologies) containing 25mM glucose, supplemented with 10% FBS, Penicillin/Streptomycin, glutamine, non-essential amino acids, 10 mM HEPES and 55 uM β-mercaptoethanol. For IL-2 addition experiments, 100 U/ml of recombinant human IL-2 (rhIL-2) was added into culture medium as indicated. RhIL-2 was obtained from the Biological Resources Branch (BRB), Division of Cancer Treatment and Diagnosis (DCTD), National Cancer Institute-Frederick Cancer Research and Development Center (NCI-FCRDC). For primary cultures, cells were treated with indicated doses of 2-deoxyglucose (2DG; Sigma) for the duration of the culture.

For secondary stimulation, after activation for 48 h in complete medium cells were harvested and washed once with PBS. And cells were re-stimulated on plates coated with anti-CD3 and anti-CD28 with indicated medium for another 48 h. Cells were treated with indicated doses of AICAR for 48 h or Compound C (Cayman Chemical) for last 24 h during re-stimulation. T_{FH} conditions designed to increase Bcl6 expression in wild-type cells by blocking the IL-2 pathway (Oestreich et al. 2012; Liao et al. 2014) used IL-6 and IL-21 (50 ng/ml each (Peprotech)), plus anti-IFNγ, -IL-2, -IL-4 and -TGF-β Abs (BioXcel), and anti-CD25, -CD122 (BD Biosciences). All neutralizing Abs used at 10 μg/mL each. EL4 cells were obtained from the laboratory of Dr. Mark Kaplan (Indiana University School of Medicine) and cultured with the indicated medium for 48 h.

Human naive CD4 T cell isolation and culture. Cryopreserved human peripheral blood mononuclear cells (PBMCs) from unidentified healthy donors were thawed in a 37°C water bath, then washed twice with pre-warmed complete RPMI 1640 culture medium. Naive CD4 T cells were isolated using the “human naive CD4 T cell isolation kit” from Miltenyi Biotech (San Diego, CA) per manufacturer’s instructions. Human T cell activation beads (anti-CD3/CD28) from Invitrogen were added at 1:1 ratio. Cells were then split into different culture conditions at the density of $5x10^5$ cells/mL, cultured in a 48-well tissue culture plate with either complete RPMI-1640 supplemented with 10% heat-inactivated fetal bovine serum (FBS) and 100 U/ml penicillin/streptomycin, or glucose-free RPMI supplemented with 10% dialyzed FBS and 100 U/ml of penicillin/streptomycin. Cells were treated with different concentrations of 2DG or AICAR and cultured in complete RPMI medium at 37 °C with 5% CO2 incubator for 4 days. For some cultures, cells were cultured in the presence of T_{FH}-skewing human recombinant cytokine cocktail (1 ng/ml of IL-12, 5 ng/ml of TGF-β, and 25 ng/ml of IL-6; all from R&D Systems), Harvested cells were subjected to both flow cytometry and Quantitative PCR (QPCR) analysis for T_{FH} cell-specific protein markers and genes respectively.

Flow cytometry reagents. Anti-mouse CXCR5 (2G8), GL7 (GL7), anti-BCL6 (K112-91) for mouse T cells and anti-TBET (4B10) were from BD Biosciences. Anti-Foxp3 (FJK-16s) and anti-mouse CD38 were from eBioscience. Anti-mouse CD4 (GK1.5), anti-mouse B220 (RA3-6B2) and anti-mouse PD-1 (29F.1A12) were from Biolegend. Anti-human CD4 (OKT4), anti-human BCL6 (BCL-UP), anti-human CD279/PD-1 (J105), anti-human CD185/CXCR5 (MU5UBEE) and fixable viability dye were purchased from eBioscience.

Cell staining for flow cytometry. After red blood cell lysis, cell suspension of total spleen cells were incubated with anti-mouse CD16/CD32 (BioXcell) for 5 minutes at room temperature, followed by surface staining for the indicated markers. For intracellular staining, after surface markers were stained, cells were fixed and stained with antibodies against transcription factors by following Foxp3 fixation kit (eBioscience) protocols. Human cells were subjected to surface staining with appropriate fluorochrome-conjugated antibodies for 30 min on ice. After wash, cells were stained with viability dye for 5 min at room temperature before fixation and permeablization 1h at room temperature followed by the intracellular staining with APC-conjugated mouse anti-BCL6 antibody 30 min in the dark. Cell events were collected on an LSR II flow cytometer (Becton Dickonson).

ELISA. Anti-NP-KLH IgG titers in serum were measured by ELISA, as previously reported (Wu et al. 2015). Briefly, 96 well Nunc-Immuno plates (Sigma-Aldrich) were coated with NP-KLH overnight at 4^{o} C. Wells were blocked with 1% BSA for 1 h and diluted serum was added and incubated at room temperature for 2 h. A peroxidase-conjugated anti-mouse IgG (Sigma-Aldrich) was used as secondary Ab. IL-2 concentrations of medium supernatants were measured with mouse IL-2 ELISA kit from BD Biosciences, following the manufacturer's protocol.

Gene expression analysis. Total RNA was prepared using the QIAGEN RNeasy Mini Kit, and cDNA was prepared with the Transcriptor First Strand cDNA synthesis kit (Roche), both following the manufacturer's protocol. QPCR reactions were carried using TaqMan™ Fast Advanced Master Mix (Applied Biosystems) with commercially available specific Taqman primers (Life Technologies). Samples were run in duplicates and the QPCR assays were run on the Applied Biosystems real-time QPCR machine. Mouse samples used *β-tubulin* (*tubb5*) as the reference gene, and human samples used *GAPDH*.

Statistical Analysis. All data analysis was done using Prism Graphpad software. Unless otherwise stated, Student t test or ANOVA with Tukey post hoc analysis were used. Only significant differences ($P < 0.05$) are indicated in Figures.

Acknowledgements

This work was supported by NIAID grants R56 AI112398 to A.L.D.

References

Andris, F., S. Denanglaire, E. Baus, A. Rongvaux, J. Steuve, R.A. Flavell and O. Leo, 2011. Metabolic stress boosts humoral responses in vivo independently of inflammasome and inflammatory reaction. J Immunol 186, 2245-2253.

Ballesteros-Tato, A., B. Leon, B.A. Graf, A. Moquin, P.S. Adams, F.E. Lund and T.D. Randall, 2012. Interleukin-2 inhibits germinal center formation by limiting T follicular helper cell differentiation. Immunity 36, 847-856.

Blagih, J., F. Coulombe, E.E. Vincent, F. Dupuy, G. Galicia-Vazquez, E. Yurchenko, T.C. Raissi, G.J. van der Windt, B. Viollet, E.L. Pearce, J. Pelletier, C.A. Piccirillo, C.M. Krawczyk, M. Divangahi and R.G. Jones, 2015. The energy sensor AMPK regulates T cell metabolic adaptation and effector responses in vivo. Immunity 42, 41-54.

Breitfeld, D., L. Ohl, E. Kremmer, J. Ellwart, F. Sallusto, M. Lipp and R. Forster, 2000. Follicular B helper T cells express CXC chemokine receptor 5, localize to B cell follicles, and support immunoglobulin production. J Exp Med 192, 1545-1552.

Carling, D., 2004. The AMP-activated protein kinase cascade--a unifying system for energy control. Trends Biochem Sci 29, 18-24.

Chang, C.H., J.D. Curtis, L.B. Maggi, Jr., B. Faubert, A.V. Villarino, D. O'Sullivan, S.C. Huang, G.J. van der Windt, J. Blagih, J. Qiu, J.D. Weber, E.J. Pearce, R.G. Jones and E.L. Pearce, 2013. Posttranscriptional control of T cell effector function by aerobic glycolysis. Cell 153, 1239-1251.

Crotty, S., 2011. Follicular helper CD4 T cells (TFH). Annu Rev Immunol 29, 621-663.

Crotty, S., R.J. Johnston and S.P. Schoenberger, 2010. Effectors and memories: Bcl-6 and Blimp-1 in T and B lymphocyte differentiation. Nat Immunol 11, 114-120.

Fazilleau, N., L. Mark, L.J. McHeyzer-Williams and M.G. McHeyzer-Williams, 2009. Follicular helper T cells: lineage and location. Immunity 30, 324-335.

Glauser, D.A. and W. Schlegel, 2009. The FoxO/Bcl-6/cyclin D2 pathway mediates metabolic and growth factor stimulation of proliferation in Min6 pancreatic beta-cells. J Recept Signal Transduct Res 29, 293-298.

Gongol, B., T. Marin, I.C. Peng, B. Woo, M. Martin, S. King, W. Sun, D.A. Johnson, S. Chien and J.Y. Shyy, 2013. AMPKalpha2 exerts its anti-inflammatory effects through PARP-1 and Bcl-6. Proc Natl Acad Sci U S A 110, 3161-3166.

Hardie, D.G., 2007. AMP-activated/SNF1 protein kinases: conserved guardians of cellular energy. Nat Rev Mol Cell Biol 8, 774-785.

Havenar-Daughton, C., S.M. Reiss, D.G. Carnathan, J.E. Wu, K. Kendric, A. Torrents de la Pena, S.P. Kasturi, J.M. Dan, M. Bothwell, R.W. Sanders, B. Pulendran, G. Silvestri and S. Crotty, 2016. Cytokine-Independent Detection of Antigen-Specific Germinal Center T Follicular Helper Cells in Immunized Nonhuman Primates Using a Live Cell Activation-Induced Marker Technique. J Immunol

Hollister, K., H. Wu, S. Kusam, N. Clegg, A. Mondal, D.V. Sawant and A. Dent, 2013. Insights into the Role of Bcl6 in Follicular Helper T Cells Using a New Conditional Mutant Mouse Model. J Immunol 191, 3705-3711

Johnston, R.J., Y.S. Choi, J.A. Diamond, J.A. Yang and S. Crotty, 2012. STAT5 is a potent negative regulator of TFH cell differentiation. J Exp Med 209, 243-250.

Johnston, R.J., A.C. Poholek, D. DiToro, I. Yusuf, D. Eto, B. Barnett, A.L. Dent, J. Craft and S. Crotty, 2009. Bcl6 and Blimp-1 are reciprocal and antagonistic regulators of T follicular helper cell differentiation. Science 325, 1006-1010.

Lee, P.P., D.R. Fitzpatrick, C. Beard, H.K. Jessup, S. Lehar, K.W. Makar, M. Perez-Melgosa, M.T. Sweetser, M.S. Schlissel, S. Nguyen, S.R. Cherry, J.H. Tsai, S.M. Tucker, W.M. Weaver, A. Kelso, R. Jaenisch and C.B. Wilson, 2001. A critical role for Dnmt1 and DNA methylation in T cell development, function, and survival. Immunity 15, 763-774.

Leon, B., J.E. Bradley, F.E. Lund, T.D. Randall and A. Ballesteros-Tato, 2014. FoxP3+ regulatory T cells promote influenza-specific Tfh responses by controlling IL-2 availability. Nat Commun 5, 3495.

Li, J., E. Lu, T. Yi and J.G. Cyster, 2016. EBI2 augments Tfh cell fate by promoting interaction with IL-2-quenching dendritic cells. Nature 533, 110-114.

Liao, W., R. Spolski, P. Li, N. Du, E.E. West, M. Ren, S. Mitra and W.J. Leonard, 2014. Opposing actions of IL-2 and IL-21 on Th9 differentiation correlate with their differential regulation of BCL6 expression. Proc Natl Acad Sci U S A 111, 3508-3513.

Linterman, M.A., R.J. Rigby, R.K. Wong, D. Yu, R. Brink, J.L. Cannons, P.L. Schwartzberg, M.C. Cook, G.D. Walters and C.G. Vinuesa, 2009. Follicular helper T cells are required for systemic autoimmunity. J Exp Med 206, 561-576.

Luo, X. and W.L. Kraus, 2012. On PAR with PARP: cellular stress signaling through poly(ADP-ribose) and PARP-1. Genes Dev 26, 417-432.

McHeyzer-Williams, L.J., N. Pelletier, L. Mark, N. Fazilleau and M.G. McHeyzer-Williams, 2009. Follicular helper T cells as cognate regulators of B cell immunity. Curr Opin Immunol

Mendez, L.M., J.M. Polo, J.J. Yu, M. Krupski, B.B. Ding, A. Melnick and B.H. Ye, 2008. CtBP is an essential corepressor for BCL6 autoregulation. Mol Cell Biol 28, 2175-2186.

Nurieva, R.I., Y. Chung, G.J. Martinez, X.O. Yang, S. Tanaka, T.D. Matskevitch, Y.H. Wang and C. Dong, 2009. Bcl6 mediates the development of T follicular helper cells. Science 325, 1001-1005.

Nurieva, R.I., A. Podd, Y. Chen, A.M. Alekseev, M. Yu, X. Qi, H. Huang, R. Wen, J. Wang, H.S. Li, S.S. Watowich, H. Qi, C. Dong and D. Wang, 2012. STAT5 protein negatively regulates T follicular helper (Tfh) cell generation and function. J Biol Chem 287, 11234-11239.

Nystrom, G.J. and C.H. Lang, 2008. Sepsis and AMPK Activation by AICAR Differentially Regulate FoxO-1, -3 and -4 mRNA in Striated Muscle. Int J Clin Exp Med 1, 50-63.

Odegard, J.M., B.R. Marks, L.D. DiPlacido, A.C. Poholek, D.H. Kono, C. Dong, R.A. Flavell and J. Craft, 2008. ICOS-dependent extrafollicular helper T cells elicit IgG production via IL-21 in systemic autoimmunity. J Exp Med 205, 2873-2886.

Oestreich, K.J., S.E. Mohn and A.S. Weinmann, 2012. Molecular mechanisms that control the expression and activity of Bcl-6 in TH1 cells to regulate flexibility with a TFH-like gene profile. Nat Immunol 13, 405-411.

Oestreich, K.J., K.A. Read, S.E. Gilbertson, K.P. Hough, P.W. McDonald, V. Krishnamoorthy and A.S. Weinmann, 2014. Bcl-6 directly represses the gene program of the glycolysis pathway. Nat Immunol 15, 957-964.

Pasqualucci, L., A. Migliazza, K. Basso, J. Houldsworth, R.S. Chaganti and R. Dalla-Favera, 2003. Mutations of the BCL6 proto-oncogene disrupt its negative autoregulation in diffuse large B-cell lymphoma. Blood 101, 2914-2923.

Poholek, A.C., K. Hansen, S.G. Hernandez, D. Eto, A. Chandele, J.S. Weinstein, X. Dong, J.M. Odegard, S.M. Kaech, A.L. Dent, S. Crotty and J. Craft, 2010. In vivo regulation of Bcl6 and T follicular helper cell development. J Immunol 185, 313-326.

Ramiscal, R.R., I.A. Parish, R.S. Lee-Young, J.J. Babon, J. Blagih, A. Pratama, J. Martin, N. Hawley, J.Y. Cappello, P.F. Nieto, J.I. Ellyard, N.J. Kershaw, R.A. Sweet, C.C. Goodnow, R.G. Jones, M.A. Febbraio, C.G. Vinuesa and V. Athanasopoulos, 2015. Attenuation of AMPK signaling by ROQUIN promotes T follicular helper cell formation. Elife 4,

Ray, J.P., M.M. Staron, J.A. Shyer, P.C. Ho, H.D. Marshall, S.M. Gray, B.J. Laidlaw, K. Araki, R. Ahmed, S.M. Kaech and J. Craft, 2015. The Interleukin-2-mTORc1 Kinase Axis Defines the Signaling, Differentiation, and Metabolism of T Helper 1 and Follicular B Helper T Cells. Immunity

Schaerli, P., K. Willimann, A.B. Lang, M. Lipp, P. Loetscher and B. Moser, 2000. CXC chemokine receptor 5 expression defines follicular homing T cells with B cell helper function. J Exp Med 192, 1553-1562.

Schmitt, N., Y. Liu, S.E. Bentebibel, I. Munagala, L. Bourdery, K. Venuprasad, J. Banchereau and H. Ueno, 2014. The cytokine TGF-beta co-opts signaling via STAT3-STAT4 to promote the differentiation of human TFH cells. Nat Immunol 15, 856-865.

Stone, E.L., M. Pepper, C.D. Katayama, Y.M. Kerdiles, C.Y. Lai, E. Emslie, Y.C. Lin, E. Yang, A.W. Goldrath, M.O. Li, D.A. Cantrell and S.M. Hedrick, 2015. ICOS coreceptor signaling inactivates the transcription factor FOXO1 to promote Tfh cell differentiation. Immunity 42, 239-251.

Sukumar, M., J. Liu, Y. Ji, M. Subramanian, J.G. Crompton, Z. Yu, R. Roychoudhuri, D.C. Palmer, P. Muranski, E.D. Karoly, R.P. Mohney, C.A. Klebanoff, A. Lal, T. Finkel, N.P. Restifo and L. Gattinoni, 2013. Inhibiting glycolytic metabolism enhances CD8+ T cell memory and antitumor function. J Clin Invest 123, 4479-4488.

Tang, T.T., D. Dowbenko, A. Jackson, L. Toney, D.A. Lewin, A.L. Dent and L.A. Lasky, 2002. The forkhead transcription factor AFX activates apoptosis by induction of the BCL-6 transcriptional repressor. J Biol Chem 277, 14255-14265.

Vincent, E.E., P.P. Coelho, J. Blagih, T. Griss, B. Viollet and R.G. Jones, 2015. Differential effects of AMPK agonists on cell growth and metabolism. Oncogene 34, 3627-3639.

Vinuesa, C.G., M.C. Cook, C. Angelucci, V. Athanasopoulos, L. Rui, K.M. Hill, D. Yu, H. Domaschenz, B. Whittle, T. Lambe, I.S. Roberts, R.R. Copley, J.I. Bell, R.J. Cornall and C.C. Goodnow, 2005. A RING-type ubiquitin ligase family member

required to repress follicular helper T cells and autoimmunity. Nature 435, 452-458.

Wang, R., C.P. Dillon, L.Z. Shi, S. Milasta, R. Carter, D. Finkelstein, L.L. McCormick, P. Fitzgerald, H. Chi, J. Munger and D.R. Green, 2011. The transcription factor Myc controls metabolic reprogramming upon T lymphocyte activation. Immunity 35, 871-882.

Wu, H., Y. Chen, H. Liu, L.L. Xu, P. Teuscher, S. Wang, S. Lu and A.L. Dent, 2016. Follicular regulatory T cells repress cytokine production by follicular helper T cells and optimize IgG responses in mice. Eur J Immunol 46, 1152-1161.

Wu, H., L.L. Xu, P. Teuscher, H. Liu, M.H. Kaplan and A.L. Dent, 2015. An Inhibitory Role for the Transcription Factor Stat3 in Controlling IL-4 and Bcl6 Expression in Follicular Helper T Cells. J Immunol

Yin, Y., S.C. Choi, Z. Xu, D.J. Perry, H. Seay, B.P. Croker, E.S. Sobel, T.M. Brusko and L. Morel, 2015. Normalization of CD4+ T cell metabolism reverses lupus. Sci Transl Med 7, 274ra218.

Yin, Y., S.C. Choi, Z. Xu, L. Zeumer, N. Kanda, B.P. Croker and L. Morel, 2016. Glucose Oxidation Is Critical for CD4+ T Cell Activation in a Mouse Model of Systemic Lupus Erythematosus. J Immunol 196, 80-90.

Yu, D., S. Rao, L.M. Tsai, S.K. Lee, Y. He, E.L. Sutcliffe, M. Srivastava, M. Linterman, L. Zheng, N. Simpson, J.I. Ellyard, I.A. Parish, C.S. Ma, Q.J. Li, C.R. Parish, C.R. Mackay and C.G. Vinuesa, 2009. The transcriptional repressor Bcl-6 directs T follicular helper cell lineage commitment. Immunity 31, 457-468.

Zeng, H., S. Cohen, C. Guy, S. Shrestha, G. Neale, S.A. Brown, C. Cloer, R.J. Kishton, X. Gao, B. Youngblood, M. Do, M.O. Li, J.W. Locasale, J.C. Rathmell and H. Chi, 2016. mTORC1 and mTORC2 Kinase Signaling and Glucose Metabolism Drive Follicular Helper T Cell Differentiation. Immunity 45, 540-554.

Zhou, G., R. Myers, Y. Li, Y. Chen, X. Shen, J. Fenyk-Melody, M. Wu, J. Ventre, T. Doebber, N. Fujii, N. Musi, M.F. Hirshman, L.J. Goodyear and D.E. Moller, 2001. Role of AMP-activated protein kinase in mechanism of metformin action. J Clin Invest 108, 1167-1174.

FIGURE LEGENDS

Figure 1. Induction of Bcl6 by blocking glycolysis. Naïve CD4+ T cells isolated from C57BL/6 mice or EL4 cells were cultured in complete (GLU+) or glucose (GLU-) deprivation medium. Cells were harvested for total RNA preparation or flow cytometric staining. (A) Relative mRNA expression was determined by quantitative RT-PCR. *Bcl6* gene expression from isolated naïve CD4+ T cells cultured under complete or glucose deprivation medium for 72 h (n=3, mean ± SEM). (B) Flow cytometry histogram plot for Bcl6 and mean fluorescence intensity (MFI) of naïve CD4+ T cells cultured under complete or glucose deprivation medium (n=3, mean ± SEM). (C) *Bcl6* gene expression from EL4 cells cultured under complete or glucose deprivation medium for 48 hours (n=3, mean ± SEM). (D) Flow cytometry histogram plot for Bcl6 and MFI of EL4 cells cultured under complete or glucose deprivation medium (n=3, mean ± SEM). (E) *Bcl6* gene expression from isolated naïve CD4+ T cells cultured under complete medium with or without 20 mM 2DG for 72 h (n=3, mean ± SEM). *$p < 0.05$, ***$p < 0.001$ (t test). Data are representative of 2 independent experiments of each time point with similar results.

Figure 2. Effects of blocking glycolysis on IL-2 and its receptor. Naïve CD4+ T cells isolated from C57BL/6 mice were cultured in complete (GLU+) or glucose (GLU-) deprivation medium for 72 h, cells were harvested for total RNA preparation and medium supernatants were collected for ELISA analysis. (A) Relative mRNA expression was determined by QPCR. *Il2ra* gene expression from T cells cultured under complete or glucose deprivation medium for 72 h (n=3, mean ± SEM). (B) *Il2* gene expression from T cells cultured under complete or glucose deprivation medium for 72 h (n=3, mean ± SEM). (C) IL-2 concentration of medium supernatants harvested from complete or glucose deprivation cell culture after 72 h (n=3, mean ± SEM). NS (not significant, $p > 0.05$, t test), ***$p < 0.001$ (t test). Data are representative of 2 independent experiments of each time point with similar results.

Figure 3. Up-regulation of BCL6 by glucose deprivation is insensitive to IL-2-mediated inhibition of Bcl6. Naïve CD4+ T cells isolated from C57BL/6 or IL-2 KO mice were cultured under complete (+GLU) or glucose (GLU-) deprivation media for 72 h, with or without addition of 100 U/ml recombinant human IL-2. Cells were harvested for total RNA preparation and relative mRNA expression was determined by QPCR. (A) *Bcl6* gene expression from C57BL/6 naïve CD4+ T cells cultured under complete or glucose deprivation medium with or without rhIL-2 addition for 72 h (n=3, mean ± SEM). (B) *Bcl6* gene expression from IL-2 KO naïve CD4+ T cells cultured under complete or glucose deprivation medium with or without rhIL-2 addition for 72 h (n=3, mean ± SEM). NS (not significant, $p > 0.05$, two-way ANOVA), ***$p < 0.001$ (two-way ANOVA). Data are representative of 2 independent experiments of each time point with similar results.

Figure 4. Up-regulation of BCL6 by glucose deprivation works with secondary re-stimulation and is specific for BCL6. Naïve CD4+ T cells isolated from C57BL/6 mice were cultured with complete media for 48 h on anti-CD3 and anti-CD28 coated plate, cells were collected and washed once with PBS and cultured under complete (GLU+) or glucose (GLU-) deprivation medium for another 48 h on anti-CD3 and anti-CD28 coated plate. Cells were harvested for total RNA preparation or flow cytometric staining. (A) Relative mRNA expression was determined by QPCR. *Bcl6* gene expression from isolated naïve CD4+ T cells cultured under complete or glucose deprivation medium during re-stimulation (n=3, mean ± SEM). (B) *Pdcd1* gene expression from isolated naïve CD4+ T cells cultured under complete or glucose deprivation medium during re-stimulation (n=3, mean ± SEM). (C) *Prdm1* gene expression from isolated naïve CD4+ T cells cultured under complete or glucose deprivation medium during re-stimulation (n=3, mean ± SEM). (D) and (E) Bcl6 MFI of naïve CD4+ T cells cultured under complete or glucose deprivation medium during re-stimulation (n=3, mean ± SEM). (F) Tbet MFI

of naïve CD4+ T cells cultured under complete or glucose deprivation medium during re-stimulation (n=3, mean ± SEM). (G) Foxp3 MFI of naïve CD4+ T cells cultured under complete or glucose deprivation medium during re-stimulation (n=3, mean ± SEM). *p < 0.05, ***p < 0.001 (t test). Data are representative of two independent experiments with similar results.

Figure 5. AMPK promotes BCL6 up-regulation, both in the presence or absence of glycolysis. (A, B) Naïve CD4+ T cells isolated from C57BL/6 mice were cultured with complete media for 48 h on anti-CD3 and anti-CD28 coated wells. T cells were collected and washed once with PBS and cultured under complete (GLU+) or glucose (GLU-) deprivation medium for another 48 h on anti-CD3 and anti-CD28 coated plate. Relative mRNA expression was determined by QPCR. (A) Different doses of Compound C were added to cells for the last 24 h of re-stimulation culture. *Bcl6* gene expression from isolated naïve CD4+ T cells cultured under complete or glucose deprivation medium with or without the addition of Compound C during re-stimulation (n=3, mean ± SEM). (B) Different doses of AICAR were added to cells for the 48 h of re-stimulation culture. *Bcl6* gene expression from isolated naïve CD4+ T cells cultured under complete medium with or without the addition of AICAR during re-stimulation. Data are representative of two independent experiments with similar results. (C-F) Naïve CD4+ T cells isolated from C57BL/6 mice were cultured with complete media for 72 h on anti-CD3 and anti-CD28 coated wells, in medium alone or Tfh conditions (IL-6+IL-21, plus anti-IL-2, IL-2Ra, anti-IL2Rb, anti-TGFb, anti-IL-4, anti-IFNg), with and without AICAR. Cells were harvested for RNA isolation and gene expression analysis by QPCR for the indicated genes. (n=3, mean ± SEM). *p < 0.05, **p < 0.01, ***p < 0.001 (two-way ANOVA).

Figure 6. AICAR enhances BCL6 and T_{FH}-dependent antibody responses *in vivo.* (A) C57BL/6 wild-type (WT) or Bcl6 cKO mice were immunized i.p. with NP-KLH or NP-KLH plus AICAR. Sera were harvested on day 14 post-immunization for NP-KLH-specific IgG titer

analysis. The X-axis shows the dilution factors. Graph shows mean ± SEM, n = 3. Data are representative of two independent experiments with similar results. (B-C) C57BL/6 mice were immunized i.p. with NP-KLH or NP-KLH plus AICAR and day 3 post immunization stained for percent T_{FH} cells (B) and Bcl6 MFI of splenic T_{FH} cells on (C). T_{FH} cells were gated as % Foxp3- PD-1^{high} CXCR5+ cells within CD4+ population. (B) n=8, mean ± SEM, from two combined experiments. (C) n=5, mean ± SEM. (D) Germinal center B cells were analyzed day 7 post immunization of C57BL/6 mice immunized i.p. with NP-KLH or NP-KLH plus AICAR. GCB cells are defined as $B220^{+}CD38^{lo}GL\text{-}7^{hi}$ cells; n=4, mean ± SEM. *p < 0.05, ***p < 0.001 (t test).

Figure 7. The AMPK pathway promotes T_{FH}-like differentiation in human CD4 T cells. Human naïve CD4 T cells were treated with 2DG **(A, B)** or AICAR **(C-F)** at the concentrations indicated, in complete (GLU+) RPMI medium containing anti-CD3/CD28 activation beads, and cultured for 4 days. In **(C, E)**, cells marked "Cytokines" were cultured with TFH skewing cytokines (IL-6, IL-12, TGFβ). **(A, B, C, E)** The expression levels of T_{FH} genes (*BCL6, CXCR5*) were analyzed by QPCR, and normalized to the levels of *GAPDH*. **(D, F)** AICAR-treated cells were subjected to surface and intracellular staining with Abs to BCL6 and PD-1. Data are the normalized results from 3 individual T cell samples and preparations. Graphs show mean ± SEM, n = 3 (two-way ANOVA). *p < 0.05 (t test).

Supplementary Figure 1.

Naïve CD4+ T cells isolated from C57BL/6 mice were labelled with Cell Trace Violet (CTV) dye and cultured in complete (GLU+) or glucose (GLU-) deprivation medium for 72 hours in anti-CD3 and anti-CD28 coated wells. Cells were harvested, fixed, stained intracellularly for Bcl6, then analyzed by flow cytometry. Gates show control staining without glucose, for reference. (A) Representative flow cytometry plots for control and Bcl6 staining. (B) Graphs of Bcl6 MFI for

total populations in (A). (C) Graphs of CTV MFI for total populations in (A). (n=3, mean ± SEM). **p < 0.01, ***p < 0.001 (t test).

Figure 1

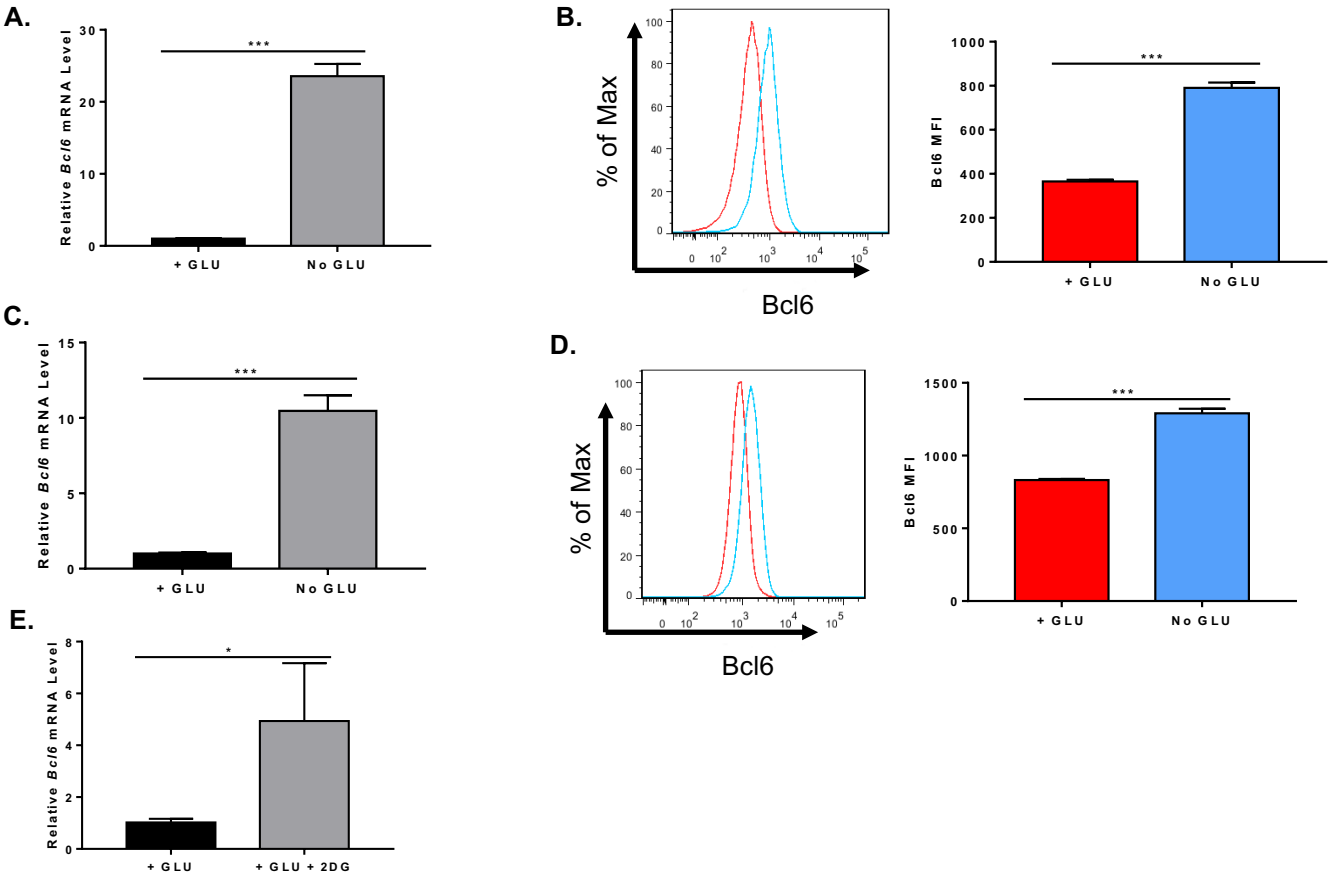
A.
Relative Bcl6 mRNA Level
30
20
10
0
***
+ GLU
No GLU
B.
% of Max
100
80
60
40
20
0
0
10^2
10^3
10^4
10^5
Bcl6
Bcl6 MFI
1000
800
600
400
200
0
***
+ GLU
No GLU
C.
Relative Bcl6 mRNA Level
15
10
5
0
***
+ GLU
No GLU
D.
% of Max
100
80
60
40
20
0
0
10^2
10^3
10^4
10^5
Bcl6
Bcl6 MFI
1500
1000
500
0
***
+ GLU
No GLU
E.
Relative Bcl6 mRNA Level
8
6
4
2
0
*
+ GLU
+ GLU + 2DG

Figure 2

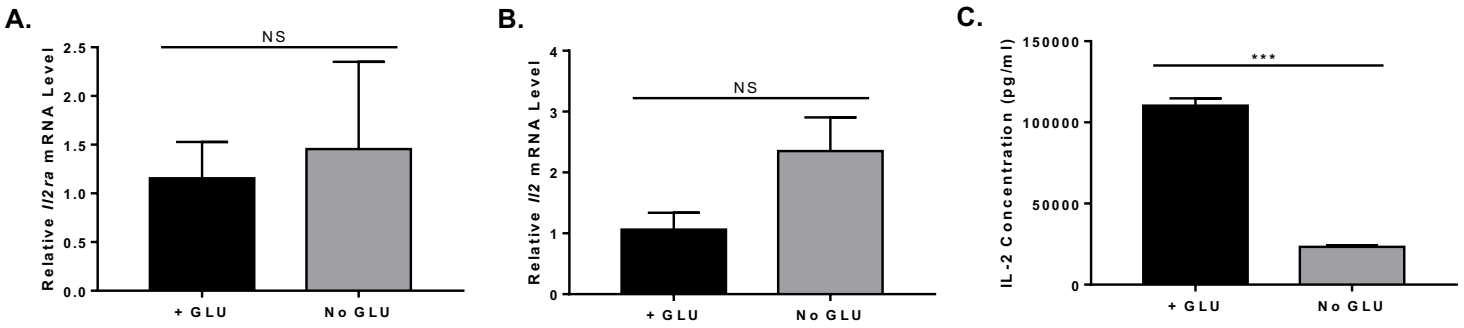
A.
NS
Relative Il2ra mRNA Level
2.5
2.0
1.5
1.0
0.5
0.0
+ GLU
No GLU
B.
NS
Relative Il2 mRNA Level
4
3
2
1
0
+ GLU
No GLU
C.
***
IL-2 Concentration (pg/ml)
150000
100000
50000
0
+ GLU
No GLU

Figure 3

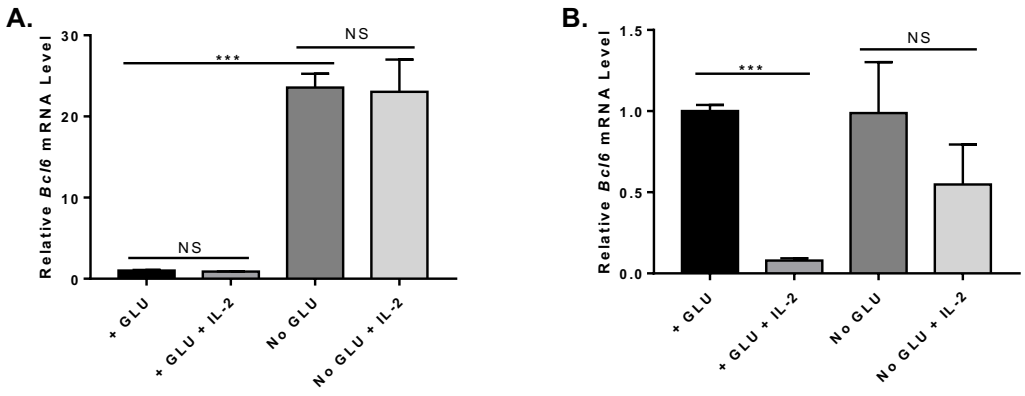
A.
Relative Bcl6 mRNA Level
30
20
10
0
***
NS
NS
+ GLU
+ GLU + IL-2
No GLU
No GLU + IL-2
B.
Relative Bcl6 mRNA Level
1.5
1.0
0.5
0.0
***
NS
+ GLU
+ GLU + IL-2
No GLU
No GLU + IL-2

Figure 4

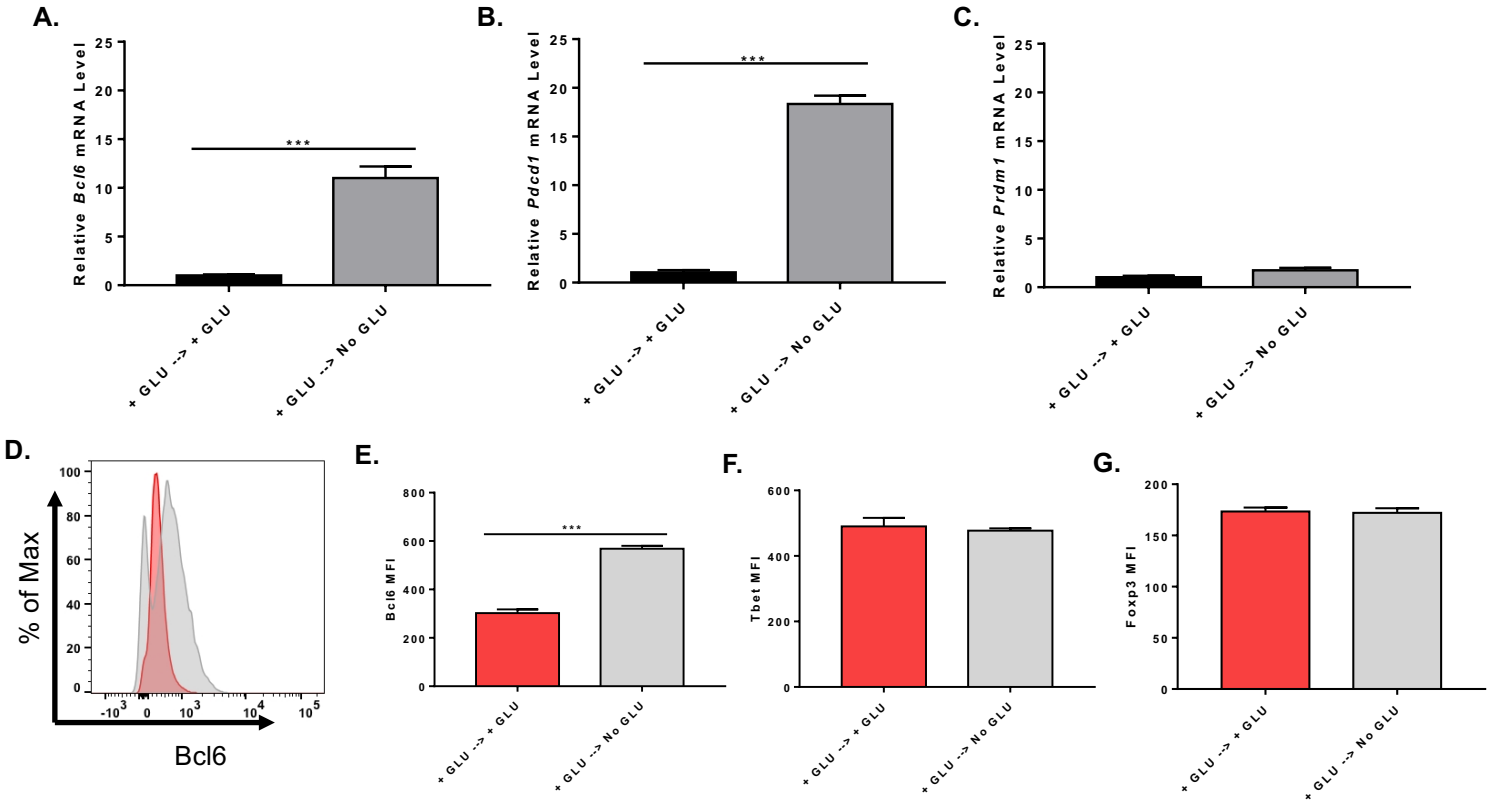
A.
Relative Bcl6 mRNA Level
25
20
15
10
5
0
***
+ GLU --> + GLU
+ GLU --> No GLU
B.
Relative Pdcd1 mRNA Level
25
20
15
10
5
0
***
+ GLU --> + GLU
+ GLU --> No GLU
C.
Relative Prdm1 mRNA Level
25
20
15
10
5
0
+ GLU --> + GLU
+ GLU --> No GLU
D.
% of Max
100
80
60
40
20
0
-10^3
0
10^3
10^4
10^5
Bcl6
E.
Bcl6 MFI
800
600
400
200
0
***
+ GLU --> + GLU
+ GLU --> No GLU
F.
Tbet MFI
600
400
200
0
+ GLU --> + GLU
+ GLU --> No GLU
G.
Foxp3 MFI
200
150
100
50
0
+ GLU --> + GLU
+ GLU --> No GLU

Figure 5

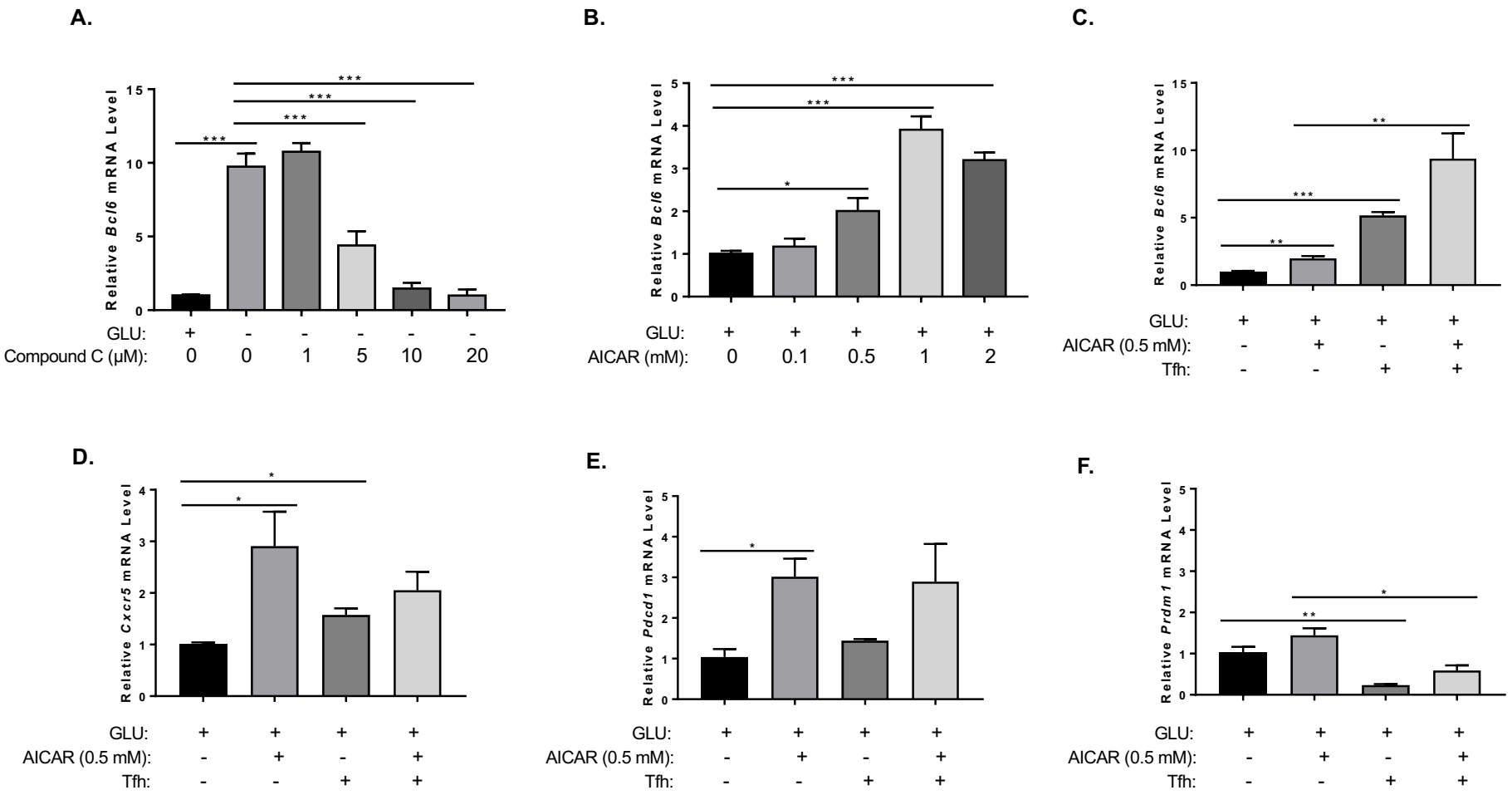
A.
Relative Bcl6 mRNA Level
GLU:
Compound C (μM):
B.
Relative Bcl6 mRNA Level
GLU:
AICAR (mM):
C.
Relative Bcl6 mRNA Level
GLU:
AICAR (0.5 mM):
Tfh:
D.
Relative Cxcr5 mRNA Level
GLU:
AICAR (0.5 mM):
Tfh:
E.
Relative Pdcd1 mRNA Level
GLU:
AICAR (0.5 mM):
Tfh:
F.
Relative Prdm1 mRNA Level
GLU:
AICAR (0.5 mM):
Tfh:

Figure 6

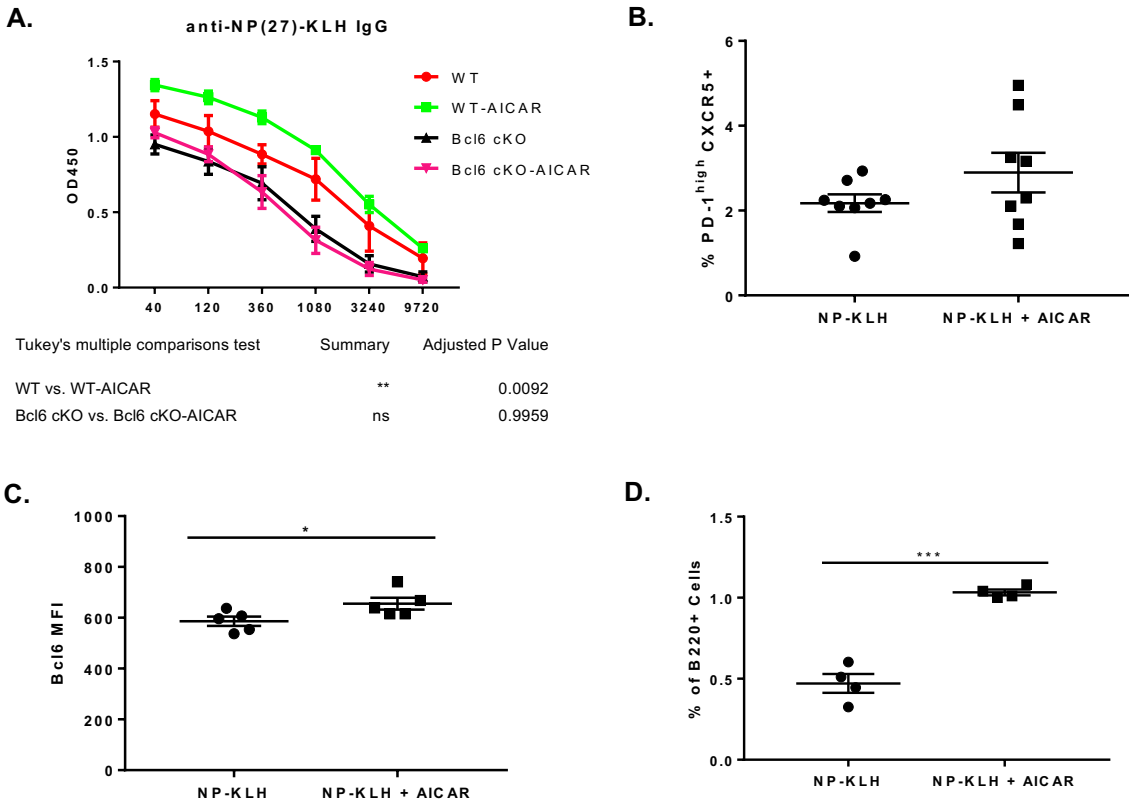
A.
anti-NP(27)-KLH IgG
OD450
1.5
1.0
0.5
0.0
40
120
360
1080
3240
9720
WT
WT-AICAR
Bcl6 cKO
Bcl6 cKO-AICAR
Tukey's multiple comparisons test
Summary
Adjusted P Value
WT vs. WT-AICAR
**
0.0092
Bcl6 cKO vs. Bcl6 cKO-AICAR
ns
0.9959
B.
% PD-1high CXCR5+
6
4
2
0
NP-KLH
NP-KLH + AICAR
C.
Bcl6 MFI
1000
800
600
400
200
0
*
NP-KLH
NP-KLH + AICAR
D.
% of B220+ Cells
1.5
1.0
0.5
0.0
***
NP-KLH
NP-KLH + AICAR

Figure 7

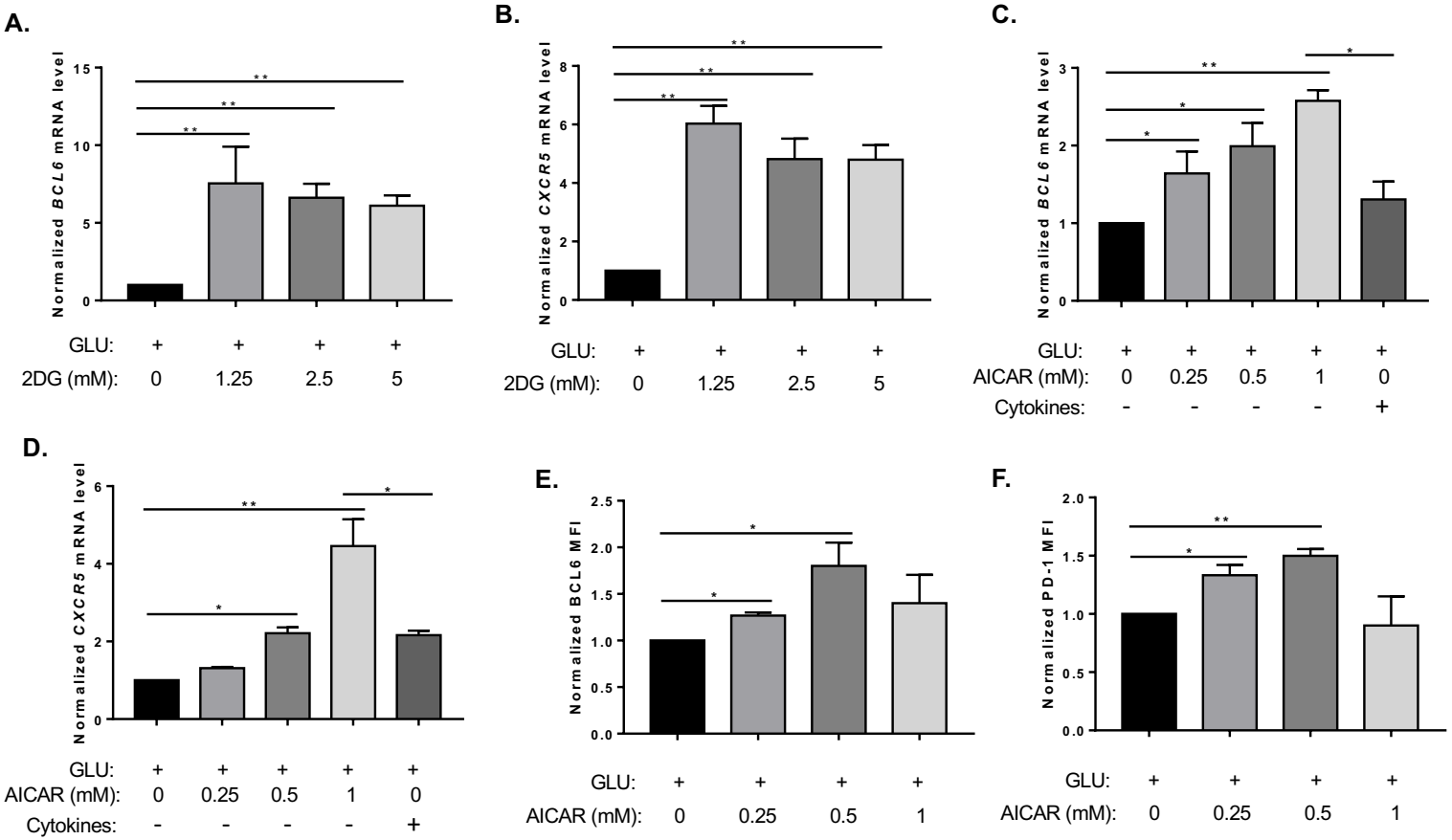
A.
Normalized BCL6 mRNA level
GLU: + + + +
2DG (mM): 0 1.25 2.5 5
B.
Normalized CXCR5 mRNA level
GLU: + + + +
2DG (mM): 0 1.25 2.5 5
C.
Normalized BCL6 mRNA level
GLU: + + + + +
AICAR (mM): 0 0.25 0.5 1 0
Cytokines: - - - - +
D.
Normalized CXCR5 mRNA level
GLU: + + + + +
AICAR (mM): 0 0.25 0.5 1 0
Cytokines: - - - - +
E.
Normalized BCL6 MFI
GLU: + + + +
AICAR (mM): 0 0.25 0.5 1
F.
Normalized PD-1 MFI
GLU: + + + +
AICAR (mM): 0 0.25 0.5 1

Supplemental Figure 1